Korean Journal of Remote Sensing, Vol.24, No.5, 2008, pp.397~408

Development and Verification of the Compact Airborne Imaging Spectrometer System

Kwangjae Lee †, Sangsoon Yong, and Yongseung Kim

Korea Aerospace Research Institute

Abstract : A wide variety of applications of imaging spectrometer have been proved using data from airborne systems. The Compact Airborne Imaging Spectrometer System (CAISS) was jointly designed and developed as the airborne hyperspectral imaging system by Korea Aerospace Research Institute (KARI) and ELOP inc., Israel. The primary mission of the CAISS is to acquire and provide full contiguous spectral information with high spatial resolution for advanced applications in the field of remote sensing. The CAISS consists of six physical units; the camera system, the gyro-stabilized mount, the jig, the GPS/INS, the power inverter and distributor, and the operating system. These subsystems are to be tested and verified in the laboratory before the flight. Especially the camera system of the CAISS has to be calibrated and validated with the calibration equipments such as the integrating sphere and spectral lamps. To improve data quality and its availability, it is the most important to understand the mechanism of imaging spectrometer system and the radiometric and spectral characteristics. The several performance tests of the CAISS were conducted in the camera system level. This paper presents the major characteristics of the CAISS, and summarizes the results of performance tests in the camera system level.

Key Words : Hyperspectral Imaging System, CAISS, Frame Rate, Radiometric and Spectral Binning.

1. Introduction

The concept of hyperspectral remote sensing began in the middle of 80's, and since then, it has been used most widely for the mapping of minerals and geography. In the early stage of hyperspectral remote sensing, geology and mineral exploration were major application fields because of the distinct spectral feature of rock and minerals that could be easily observed with hyperspectral remote sensing (Kim, 2005). Recently, with technology advancement, imaging spectrometer has begun to focus on wide variety of earth science applications. Hyperspectral remote sensing is a relatively new technology that is currently being investigated by researchers and scientists with regard to the detection and identification of minerals, vegetation, and man-made materials. Hyperspectral remote sensing has been used to detect and map a wide variety of materials based on characteristic reflectance spectra. For example, hyperspectral image data have been used by geologists for mineral mapping (Clark *et al.*, 1992,

Received August 4, 2008; Revised September 26, 2008; Accepted October 6, 2008.

† Corresponding Author: Kwangjae Lee (kjlee@kari.re.kr)

1995) and to detect soil properties (Ben-Dor *et al.*, 2002). Scientists have successfully used hyperspectral image data to study plant canopy chemistry (Aber *et al.*, 1995), study vegetation mapping and wildfire fuel mapping (Drake *et al.*, 1999; Roberts *et al.*, 2003; Yoon *et al.*, 2007), estimate forest leaf area index (Gong *et al.*, 2003), and detect vegetation stress (Merton, 1999).

A wide variety of applications of imaging spectrometer have been proved using data from airborne systems. With the recent appearance of commercial airborne hyperspectral imaging systems such as the CASI (Canada), AISA (Finland), and HYMAP (Australia), hyperspectral imaging is poised to enter the mainstream of remote sensing. The hyperspectral image data have been gradually expanding the usage to the fields of forest, agriculture, water resources, and military because the multispectral image data were not very effective to extract the available spectral information compare to hyperspectral image data. Most of multispectral imaging systems with high resolution such as IKONOS and QuickBird can only produce images with a few relatively broad wavelength bands. On the other hand, hyperspectral imaging systems collect the image data simultaneously in many narrow, adjacent spectral bands. These measurements make it possible to derive continuous spectrum information for each image cell. Most of the airborne hyperspectral imaging systems have the ability to control the spectral configuration of the imaging instrument. Hyperspectral image data are generally composed of about 100 to 200 spectral bands in relatively narrow bandwidths (5-10 nm), whereas multispectral image data are usually composed of about 5 to 10 bands in relatively large bandwidths (70-400 nm). However, in order to fully use the hyperspectral image data for various applications, it is necessary that imaging system with related subsystems shall be calibrated and validated in the laboratory (Lee, 2007). The radiometric and spectral performance and properties are the most important factors for the hyperspectral imaging system. So the imaging instrument which is an on-board camera system of airplane has to be checked and verified with calibration equipments in the ground level. The basic concept of calibration and validation for the airborne imaging systems is quite similar to spaceborne sensors.

In this paper, we introduce the Compact Airborne Imaging Spectrometer System (CAISS) which was developed as the airborne hyperspectral imaging system. The CAISS is the high performance imaging spectrometer system which is to meet full contiguous spectral requirement for advanced applications. The purpose of this study is to verify the radiometric and spectral performance and requirement of the camera system on the CAISS. To fulfill this purpose, the several performance tests of the CAISS were conducted with the calibration equipments such as the integrating sphere and spectral lamps in the camera system level. This paper describes the major characteristics of the CAISS and summarizes the results of performance tests in the camera system level.

2. The Compact Airborne Imaging Spectrometer System

1) System Overview

The CAISS was jointly designed and developed as the hyperspectral imaging system by Korea Aerospace Research Institute (KARI) and ELOP inc., Israel. The primary mission of the CAISS is to acquire and provide full contiguous spectral information with high spatial resolution for advanced applications in the field of remote sensing. The CAISS, as shown in Fig. 1, consists of six physical

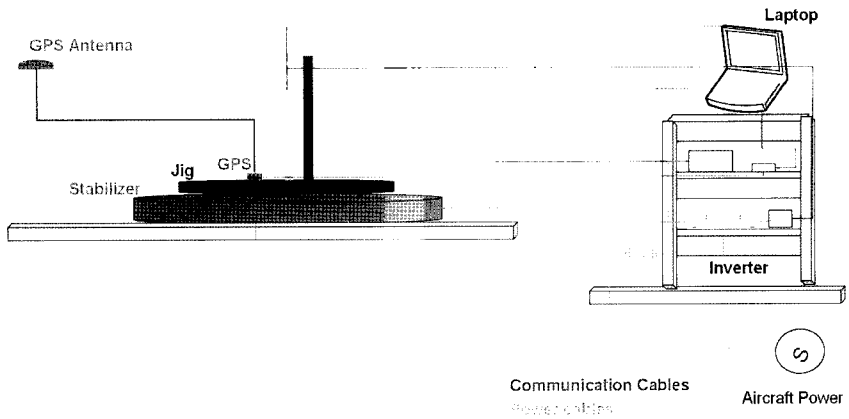

Fig. 1. The CAISS configuration.

units; the camera system, the gyro-stabilized mount, the Jig, the GPS/INS, the power inverter and distributor, and the operating system.

The camera system of the CAISS is based on the DALSTAR 1M30 digital camera which is made by DALSA, Canada and ImSpector V10E imaging spectrograph which is made by SPECIM, Finland. The camera system has the ability to control the spectral configuration of the instrument and define for each band its center line. Changing the flight altitude will change the Ground Sample Distance (GSD) and we would have the ability to simulate images with spectral and spatial resolutions similar to other sensors.

In order to compensate for the rotations of airplane during the imaging and to protect the camera system, the gyro-stabilized mount is necessary. Also special adapter such as the jig is necessary to mount the camera system on top of the gyro-stabilized mount. The GPS is assembled on top of the Jig. The GPS antenna is to be attached on airplane's outside. Since most of the airplane provides a Direct Current (DC) power source, therefore the power inverter shall be prepared to stable supply the Alternating Current (AC) power to the CAISS subsystem. A laptop will be used as the main operating system so that the peripheral interface between a laptop and the CAISS subsystem is connected by communication cables as shown in Fig. 1. Also, the software for operating the

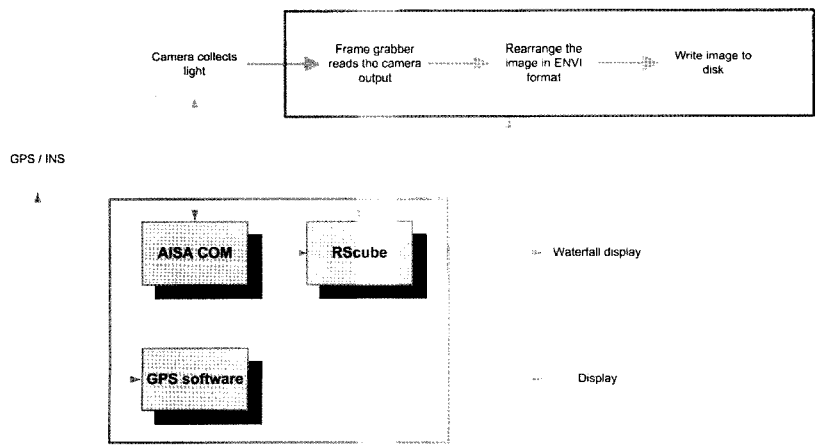

Fig. 2. The CAISS operation workflow during the mission.

subsystems is certainly necessary during the mission. Fig. 2 shows the necessary software and workflow of system operation for imaging during the flight. However, different software shall be used for each of the camera system operation, GPS/INS operation, data pre- and post-processing.

2) The camera system of the CAISS

The camera system of the CAISS in Fig. 3 consists of the DALSTAR 1M30 digital camera, the ImSpector V10E imaging spectrograph, the PCI frame grabber, the power supply, and cables.

The imaging instrument which is an on-board camera system of airplane is the most important component for hyperspectral imaging system. In order to meet the top level requirements regarding number of bands, wavelength, bandwidth, and spatial resolution, the DALSTAR 1M30 digital camera and ImSpector V10E imaging spectrograph were selected as the CCD detector and spectrometer.

The DALSTAR 1M30 digital camera provides high-sensitivity images with 1k x 1k spatial resolution. The 1M30 is a frame transfer CCD camera using a progressive scan CCD to simultaneously achieve outstanding resolution and gray scale characteristics (DALSA, 2001). The number of spatial pixels is 512 pixels and pixel size is 12 mm. Attached to the camera, there is an ImSpector V10E image spectrograph that disperses the light coming from the fore optics into more than 60 spectral lines. The spectrograph disperses the light across the CCD lines in such a way that the instrument works as a line scanner in push-broom mode. For every line in the scene, the spectrograph disperses the light so that the spectrum is sampled instantaneously. Subsequently, the camera system of the CAISS provides full contiguous spectral information with high quality spectral and spatial resolution.

The camera system has a spatial binning mechanism which is essentially aggregating pixels at detector level. Data can be spatially binned by 2 to provide 512 pixels. Also spectral binning can aggregate several spectral bands together. This is usually done at the detector level to reduce noise. Fig. 4 shows the spectral binning mechanism of the camera system on the CAISS. A Full Width Half Maximum (FWHM) is an expression of the extent of a function, given by the difference between the two extreme values of the independent variable at which the dependent variable is equal to half of its maximum value. The FWHM in Fig. 4 is the spectral width of sources. However, as shown in Fig. 4, the bandwidth

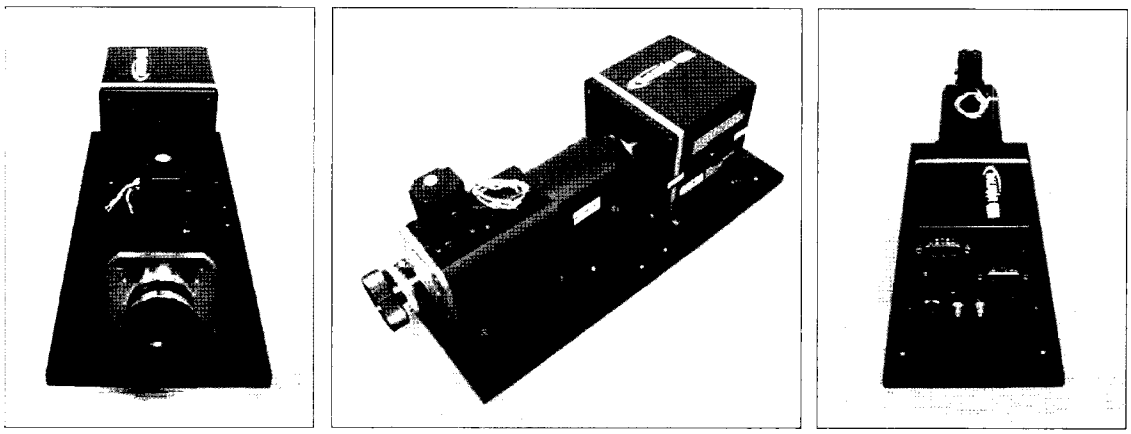

Fig. 3. The camera system of the CAISS.

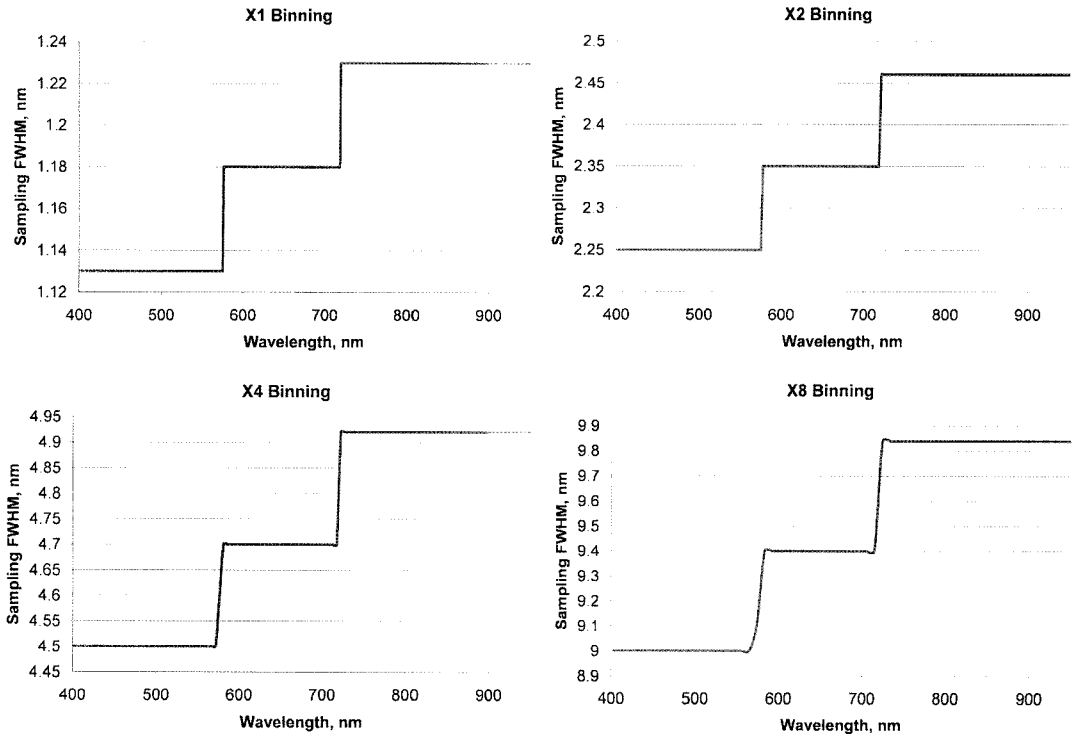

Fig. 4. The spectral binning of 1, 2, 4, and 8.

is different according to the wavelength because the spectral binning is performed at detector level.

The major specifications of camera system are as follows; the system Field of View (FOV) is 39.6 degree. The spectral range is almost 400 nm to 950 nm. The minimum spectral resolution is 1.25 nm for 480 bands and maximum spectral resolution is 10 nm for 60 bands. Swath and GSD is almost 2,070 m and 4 m at 3,000 m altitude. Radiometric resolution is 12 bits. The frame system is capable to work with frame rates of up to 43 Hz. It is controlled by a command. Frame rate is defined as the time period between the first frame to the next. Since altitude is directly connected to the spatial resolution we could calculate and plot a graph relating altitude and frame rate for several ground speeds. Fig. 5 shows the results of relationship between altitude and frame rate in the spatial binning of 1 and 2. Since the focal length of

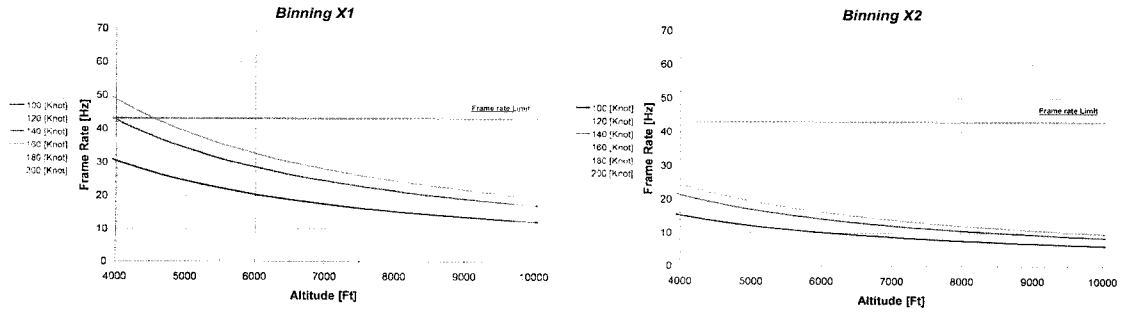

Fig. 5. Relationship between altitude and frame rate.

the camera is fixed, any change in altitude would immediately effect the spatial resolution.

Integration time is the time in which the camera collects light. It starts with the frame rate and ends according to the user definition. The integration time is usually shorter than the frame rate time. The camera system of the CAISS has the ability to change the integration time without changing the frame rate, within the limits of the frame rate time.

3) Gyro-stabilized Mount

The gyro-stabilized mount is a platform for devices used in airborne imaging system. The mission of gyro-stabilized mount is to have stable support for the aerial equipments and to compensate for the rotations (roll, pitch, and yaw movements) of the airplane during the imaging. The advantages of gyro-stabilized mount for airborne imaging system are the drastic reduction of angular rates that are caused by turbulences in the atmosphere, and elimination of momentary roll, pith, and yaw angle errors.

After full considerations based on the requirement of design stage in stability, sensing rate range, and self test function, we finally decided to accept the GSM 3000.

The major specifications of gyro-stabilized mount are as follows; the angular stabilization ranges are $\pm$ 5 degree (arbitrary horizontal axis), $\pm$8.4 deg (pitch at 0 degree roll), $\pm$6.2 degree (roll at 0 deg pitch), and $\pm$25 degree (yaw), the compensable angular rate is 15 deg/sec, the residual angular rate of the horizontal axes is less than 0.2 degree/sec rms, the compensable angular accelerations are $\geq$110 degree/s^2(at a residual angular rate of $\leq$0.3 degree/sec rms) and $\geq$300 degree/s^2(at a residual angular rate of $\leq$1 degree/sec rms), mass is approximately 35 kg (SOMAG AG, 2006).

The GSM 3000 provides a stabilized platform in all three rotational axes. Instead of using mechanical gimbals and complex gear drives, roll and pitch stabilization is done by a hydraulic system consisting of four cylinders and two servo pumps. A third control loop compensates the drift angle of the airplane, and dynamically gyro-stabilizes deviations from heading using classic gear drives and bearings. The GSM 3000 platform mainly consists of four different groups of functionality; the base plate, the main body, the suspension ring, and passive vibration insulation ring. Fig. 6 shows the simplified structure and picture of the gyro-stabilized mount GSM 3000.

In the Fig. 7, the adapter plate is a specially manufactured jig that assembles the camera system to

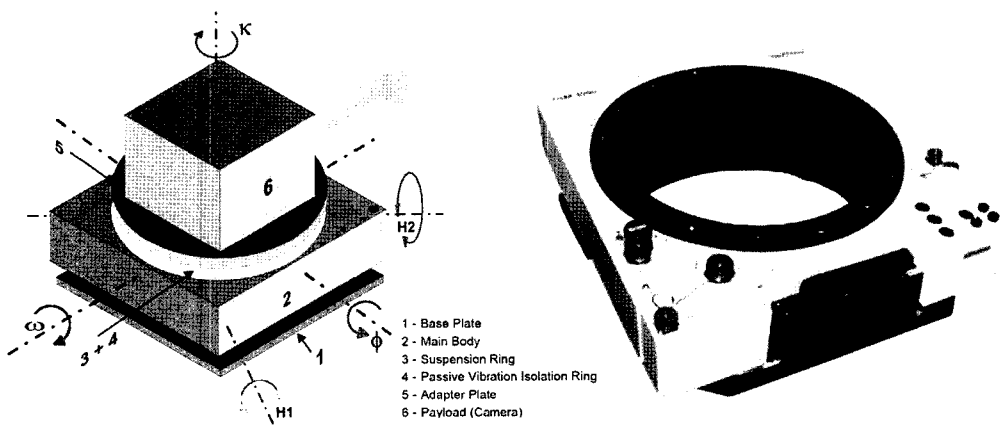

Fig. 6. The structure and picture of the gyro-stabilized mount GSM 3000.

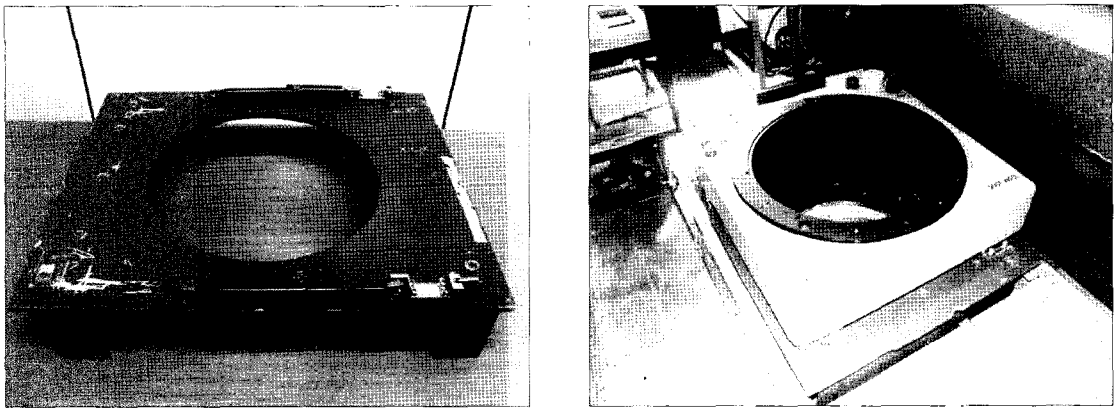

Fig. 7. The special adapter for assembling the gyro-stabilized mount on the airplane floor.

the passive vibration insulation ring. Another special adapter in the Fig. 7 is also necessary to assemble the base plate of the gyro-stabilized mount to the window of the airplane floor. Fig. 7 shows the assembled result between the gyro-stabilized mount and airplane floor using the specially manufactured adapter. But this adapter is changeable item, depending on the airplane type and condition of airplane floor.

4) Jig

The main mission of the jig in the CAISS is to mount the camera system on top of the gyro-stabilized mount. So the jig was designed and manufactured as shown in Fig. 8 according to the gyro-stabilized mount that was used the CAISS. The jig contains an adapter plate for alignment and fixation of the camera system. After assembling the GPS and camera system to the Jig, it is mounted on top of the gyro-stabilized mount.

5) GPS/INS

The GPS/INS is one of the important components for airborne imaging system. In the CAISS, MIDG II which is made by Microbotics Inc. will be used because it provides full Inertial Navigation System (INS) solution with low power, light weight, and small size. The MIDG II is a GPS aided INS for use in applications requiring attitude, position, velocity, acceleration, and angular rates for navigation or control. An internal GPS receiver measures position and velocity and passes it to the data fusion processor to be combined with the inertial data to generate an

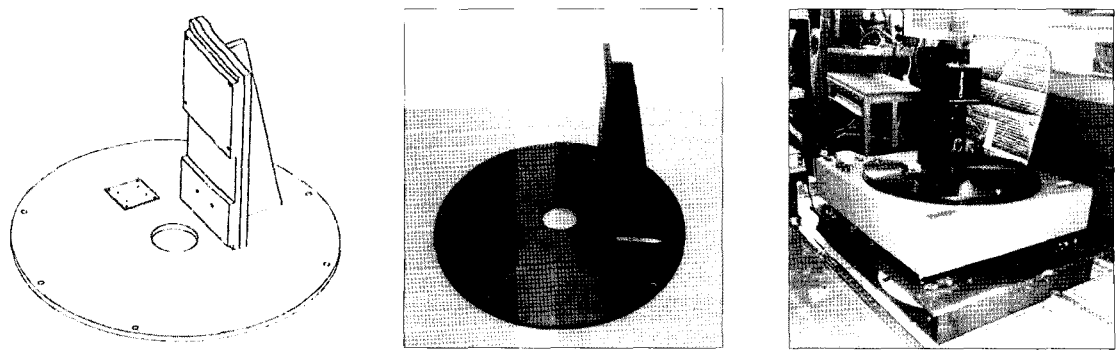

Fig. 8. Assembly of the camera system and gyro-stabilized mount using the jig.

optimal solution.

For specifications, the position accuracy of MIDG II is 2m CEP (WAAS/EGNOS available), angular rate range is ±300 degree/sec, attitude accuracy (tilt) is 0.4 degree, a data output rate of position, velocity, attitude, rates, and accelerations is 50 Hz. Raw GPS measurements rate is 5 Hz (WAAS/EGNOS) (Microbotics Inc., 2005). GPS receiver provides a self test mechanism and test results through defined interface. The GPS receiver is communicated with computer via RS422 interface. The power of GPS receiver is supplied by separated connector interface.

6) Power Inverter and Distributor

The power inverter is necessary to convert a DC power source to AC power for the CAISS operation during the flight because most of airplane only provides a DC power source. The DC power cable on the airplane will be directly connected with the power inverter. After converting the power, the AC power will be transmitted to each subsystem through the power distributor.

7) Operating System

The operating system consists of the computer system and software. The computer system is based on a laptop computer with windows XP. The peripheral interface for the GPS/INS control, the camera system operation, and the image data reception is defined. For example, the image data receiving interface is based on the PCMCIA card. The real-time imaging data will be directly recorded on the hard disk of laptop. It is also possible to use the external hard disk for real-time data storage during the imaging.

A different type of software has to be used for each camera system operation, GPS/INS operation, data pre- and post-processing. First of all, three kinds of software that are provided by camera manufacturer shall be used for operating the camera system. The Bandage, the AISA COM, and the RSCube software shall be used step by step. The Bandage software defines and creates the spectral band configuration for the mission such as Fig. 9. The AISA COM is responsible for communicating with the camera system. The purpose of AISA COM is to control the system parameters such as the frame rate, integration time, and binning level. These parameters can be changed any time through out the mission. The RSCube in Fig. 9 is the camera operation software for the imaging. It will be used to monitor the camera performance and check a real-time display of what is being imaged during the mission.

Related to the GPS/INS, the MIDG II Sync and the MIDG II software shall be used. The purpose of MIDG II Sync software is to synchronize time

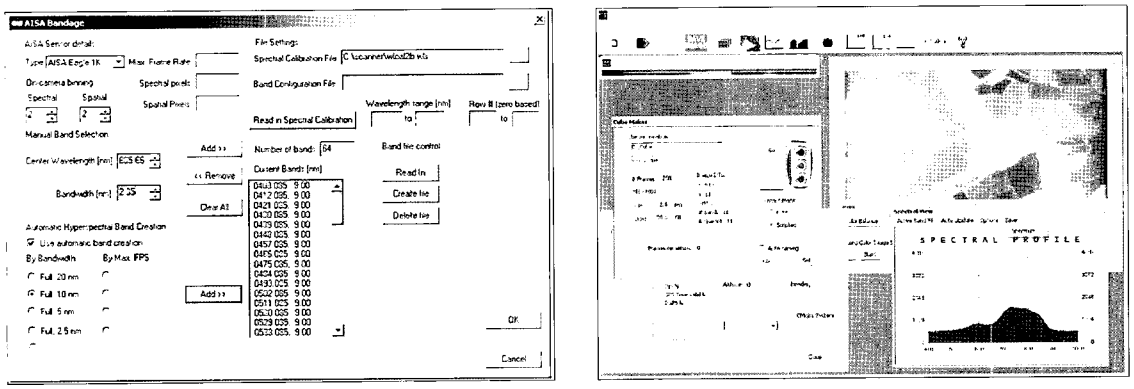

Fig. 9. The Bandage software (left) and the RSCube software (right).

between laptop time data and GPS/INS time data. Likewise MIDG II facilitates immediate access to the MIDG II data for evaluation and test.

Meanwhile, the CaliGeo software and COTS software such as ENVI will be used for data pre- and post-processing. Radiometric and geometric correction and synchronization of image data to the GPS/INS data should be done by the CaliGeo software with calibration file, dark image, band configuration file, and GPS/INS files.

3. Verification of Radiometric and Spectral Characteristics

1) Calibration Equipments

The calibration equipments are not part of the CAISS. However, these equipments are an essential component of any imaging instruments. Fig. 10 shows the prepared calibration equipment for the camera system of the CAISS.

The radiometric and spectral calibration and validation of the camera system are performed with the integrating sphere and spectral lamps in the laboratory. In this study, the medium integrating sphere uniform source system which is designed to provide exceptional uniform luminance was used for the test and calibration of the camera system. This system has the ability to provide stepped luminance output or continuous output. The wavelength spectrum is 300-2400 nm, luminance uniformity is better than 98% (percents), diameter of sphere, and exit ports are 12 inches and 4 inches (Labspere Inc., 2006). The integrating sphere provides the capability of the National Institute of Standards and Technology (NIST) traceable luminance calibration.

In the meantime, the purpose of spectral verification is to evaluate the camera system spectral response to be similar as of the spectral lamps. Four different spectral lamps (HgNe, Krypton, Xenon and Neon) are used for the spectral verification of the camera system.

2) Radiometric analysis

The preliminary radiometric calibration and validation were conducted during the CAISS Acceptance Test (AT) in the laboratory, Israel. The data consists of dark and light image in a length of 300 lines over the whole field of view of the camera. These images were taken for spatial binning of 1 and 2 and spectral binning of 1, 2, 4, and 8, thus giving 8 different binning combinations. For each binning combination 10 pairs of dark and light images were

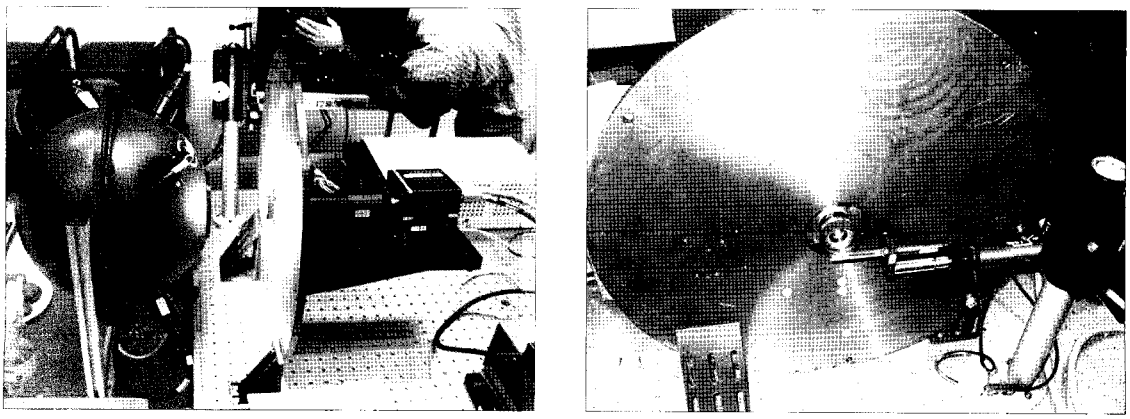

Fig. 10. The calibration equipments for the CAISS.

acquired. For each pair of images, the calibration coefficient was calculated by the calibration program. The calibration would be done according to the following equation:

$$CalibrationCoefficient_{(x,\lambda)} = \frac{\mathrm{Rad}_{\lambda} \times \mathrm{I.T}}{(\mathrm{Img}_{(x,\lambda)} - \mathrm{dark}_{(x,\lambda)})} \quad (1)$$

where,

Calibration $\mathrm{Coefficient}_{(x,\lambda)}$: the calibration coefficient for each spatial $\mathrm{pixel}_{(x)}$ and each $\mathrm{wavelength}_{(\lambda)}$

Rad_{λ} : the radiometric value of the integrating sphere flat field

$\mathrm{Img}_{(x,\lambda)}$: the integrating sphere flat field image from the CAISS

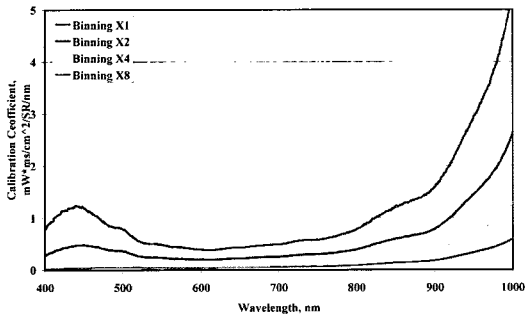

Fig. 11. Calibration coefficients for spatial binning of 1 and spectral binning of 1, 2, 4, and 8.

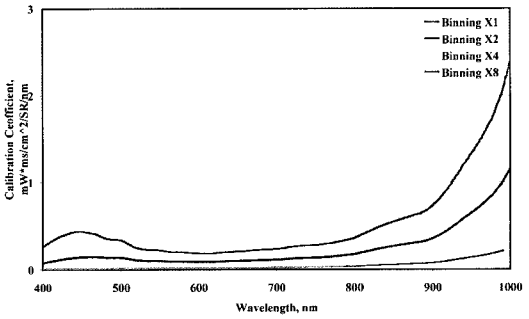

Fig. 12. Calibration coefficients for spatial binning of 2 and spectral binning of 1, 2, 4, and 8.

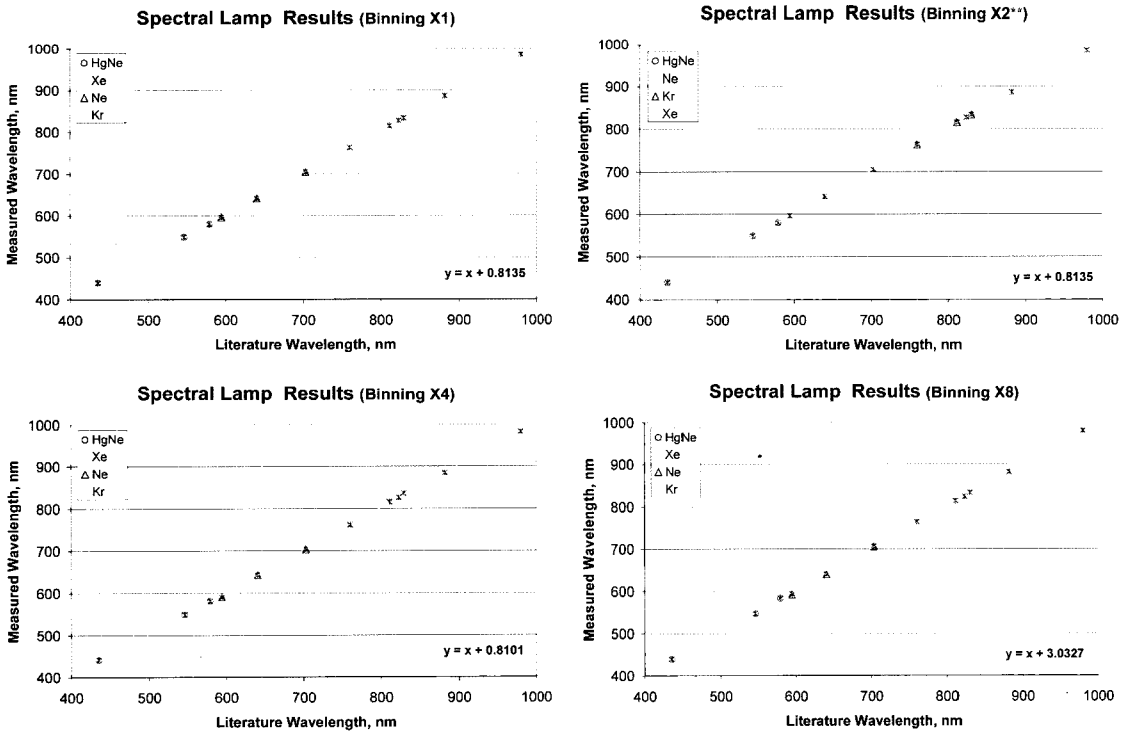

Fig. 13. Comparison of the measured wavelength from spectral lamps and the literature wavelength on the data sheet for each of the binning (**Dark image of XE lamp in the binning of 2 was simulated using the acquired dark image from the binning of 4 because of the system error.).

$Dark_{(x,\lambda)}$: the dark image from the CAISS

I.T. : the integration time for acquiring the dark image and flat filed image

The ten calibration coefficients were calculated for each of the binning combination as described above. Fig. 11 and Fig. 12 show the results of radiometric calibration coefficients. The error between the various calibration coefficients was calculated by dividing the STD by the average of the ten calibration coefficients. Error between the ten calibration coefficients was smaller than 0.3% for all calibration coefficients for the various spatial and spectral binning.

3) Spectral analysis

Four spectral lamps (HgNe, Krypton, Xenon, and Neon) were used for verifying the spectral characteristic of the camera system. The 300 frames of the lamps illumination and a dark image were acquired from the camera system. For each of the spectral lamp, all four binning (x1, x2, x4, and x8) were measured using the lamps. To subtract the dark signal from the image, according to the following equation:

$$\text{Dark Corrected Signal} = \overline{\text{Image}} - \overline{\text{Dark Image}} \quad (2)$$

where,

Dark Corrected Image: the image

Image : the average in signal of the spectral lamps image acquired by the camera system for each spatial pixel

Dark Image: the average dark signal of the camera system in each spatial pixel

The peaks of each lamp in the spectral profile of three spatial pixels were found. Then, the position of the peaks was compared to the spectral lamps data sheet. For all measurements, it was found that the spectral deviation was lower than the FWHM of the system for each of the binning. Fig. 13 shows the results from comparison of the measured wavelength from spectral lamps and the literature wavelength on the data sheet for each of the binning.

4. Summaries

This paper presents the major characteristics of the CAISS which was developed as the airborne hyperspectral imaging system and summarizes the preliminary results of performance tests in the camera system level during the acceptance test. The CAISS is the high performance imaging spectrometer system which is to meet full contiguous spectral requirement with high spatial resolution for advanced applications in the field of remote sensing. However, it is necessary that the camera system of the CAISS is calibrated and validated periodically with the calibration equipments such as the integrating sphere and spectral lamps for maintenance of radiometric and spectral properties. The preliminary test and analysis for verification of radiometric and spectral characteristics were conducted during the acceptance test in Israel. For the radiometric calibration and validation, ten pairs of dark and light images were acquired for spatial binning of 1 and 2 and spectral binning of 1, 2, 4, and 8. The ten calibration coefficients were calculated for each of the binning combinations. The error between the ten calibration coefficients was smaller than 0.3% for all calibration coefficients for the various spatial and spectral binning. In order to verify the spectral characteristics, four spectral binning (x1, x2, x4, and x8) were measured using each of the spectral lamps and the position of the peaks was compared to the reference data sheet of each spectral lamps. For all measurements, it was found that the spectral deviation was lower than the FWHM of the system for each of the binning. However, calibration and validation for the camera system of the CAISS will be conducted

once again before the flight test in Korea.

References

Aber, J. D., and M. E. Martin, 1995. High spectral resolution remote sensing of canopy chemistry. In Summaries of the Fifth JPL Airborne Earth Science Workshop, JPL Publication 95-1, v.1, 1-4.

Ben-Dor, E., K. Patin, A. Banin, and A. Karnieli, 2002. Mapping of several soil properties using DAIS-7915 hyperspectral scanner data-a case study over clayey soils in Israel. *International Journal of Remote Sensing*, 23(6): 1043-1062.

Clark, R. N., and G. A. Swayze, 1995. Mapping minerals, amorphous materials, environmental materials, vegetation, water, ice, and snow, and other materials: The USGS Tricorder Algorithm. In Summaries of the Fifth Annual JPL Airborne Earth Science Workshop, JPL Publication 95-1, v.1, 39-40.

Clark, R. N., G. A. Swayze, and A. Gallagher, 1992. Mapping the mineralogy and lithology of Canyon lands, Utah with imaging spectrometer data and the multiplespectral feature mapping algorithm. In Summaries of the Third Annual JPL Airborne Geoscience Workshop, JPL Publication 92-14, v.1, 11-13.

DALSA, 2001. DALSTAR 1M30P user's manual and reference.

Drake, N. A., S. Mackin, and J. J. Settle, 1999. Mapping vegetation, soils, and geology in semiarid shrublands using spectral matching and mixture modeling of SWIR AVIRIS imagery. *Remote Sensing of Environment*, 68: 12-25.

Gong, P., R. Pu, G. S. Biging, and M. R. Larrieu, 2003. Estimation of forest leaf area index using vegetation indices derived from hyperion hyperspectral data. *IEEE Transaction Geoscience and Remote Sensing*, 41(6): 1355-1362.

Labspere Inc., 2006. Uniform source systems manual.

Lee, K., S. Yong, and Y. Kim, 2007. Design and development of the compact airborne imaging spectrometer system. *Proceedings of International Symposium on Remote Sensing 2007*, 118-121.

Merton, R. N., 1999. Multi-temporal analysis of community scale vegetation stress with imaging spectroscopy. Ph.D. Thesis, Geography Department, University of Auckland, New Zealand, 492p.

Microbotics Inc., 2005. MIDG II specification manual.

Roberts, D. A. and P. E. Dennision, 2003. Hyperspectral technologies for wildfire fuel mapping. Proc. 4th International Workshop on RS and GIS Applications to Forest Fire Management, pp.66-75.

SOMAG AG, 2006. Gyro-stabilized mound GSM 3000 manual.

Spectral Imaging Ltd., 2007. ImSpector V10E data sheet.

Yoon, Y. and Y. Kim, 2007. Application of hyperion hyperspectral remote sensing data for wildfire fuel mapping, *Korean Journal of Remote Sensing*, 23(1): 21-32.